Magnetic properties of small cobalt–copper clusters

2013 J. Phys.: Condens. Matter 25 216003

(http://iopscience.iop.org/0953-8984/25/21/216003)

J. Phys.: Condens. Matter **25** (2013) 216003 (7pp) doi:10.1088/0953-8984/25/21/216003

Magnetic properties of small cobalt–copper clusters

G Martínez[1], E Tangarife[2], M Pérez[2] and J Mejía-López[2,3]

[1] Instituto de Física, Universidade Federal do Rio Grande do Sul, 91501-970 Porto Alegre, RS, Brazil
[2] Facultad de Física, Pontificia Universidad Católica de Chile, Avenida Vicuña Mackenna 4860, Santiago, Chile
[3] Center for the Development of Nanoscience and Nanotechnology (CEDENNA), 917-0124 Santiago, Chile

E-mail: martinez@if.ufrgs.br

Received 6 November 2012, in final form 6 March 2013
Published 3 May 2013
Online at stacks.iop.org/JPhysCM/25/216003

Abstract
Accurate first-principle calculations on bimetallic cobalt–copper clusters of up to six atoms (Pérez *et al* 2012 *J. Nanopart. Res*. **14** 933) revealed a close similarity of the ground-state magnetic properties to the ultimate jellium model, provided that a 2D to 3D geometric transition was invoked. We discuss this relationship in terms of partial occupancies of the valence electrons in both cases, with the jellium results described by nonperturbative spherical wavefunctions. Based upon this, we propose a scheme to predict magnetic properties of cobalt–copper clusters of up to twenty atoms using arguments of dimensionality and charge localization, and confirm some of these results with other independent density-functional calculations and experimental available data. The comparison with experiments is carried out for neutral and singly ionized cobalt clusters. Furthermore, a many-body tight-binding pseudopotential is used with Monte Carlo techniques to verify the stability of these new first-principle solutions.

(Some figures may appear in colour only in the online journal)

1. Introduction

Magnetic properties of small clusters are strongly linked to their structures. The case of bimetallic transition metal clusters is even more intricate, due to partially filled d-shells. Very little is known about nanoclusters of Co–Cu and there is strong interest in studying their properties because of forecast applications in magnetic storage, nanocatalysis, and nanoelectronics [1]. The Co–Cu system is also investigated because of unusual giant magnetoresistive bulk properties [2]. Concerning Co–Cu clusters, a principal interest in the area is the use of parameters to control their physical properties, a tough problem since the electron distribution in nanostructures is a complex phenomenon that grows exponentially with the cluster size. Diverse aspects like dimensionality, structural geometry, charge localization, chemical bonding, atomic segregation, and large isomeric degeneracies come into this equation. Therefore, any predicted behavior of these magnetic clusters is very much appreciated.

In this study we deal with this problem using a combination of tools, involving first-principle calculations of the valence electrons of small cobalt–copper clusters [3], its relationship to the ultimate jellium model [4, 5], an empirical prediction up to 20 atoms for all stoichiometries, as described in this work, a Monte Carlo study of a many-body potential to fit the *ab initio* results, and a comparison with experimental results [6, 7]. The latter is a definite test on this subject and we include discussion for neutral and ionized Co clusters.

Since the early work by Dunlap [8, 9], the relationship between structure and magnetism in clusters has been sought to the highest level (see, for example, [10, 11]). The case of Co–Cu nanoclusters has been dealt with by so many authors that we cannot mention them all. Here, we refer to the works by Wang *et al* [12], Ju *et al* [13], and Lu *et al* [14], where evidence of phase segregation was found in small Co–Cu clusters. There are, however, only a few

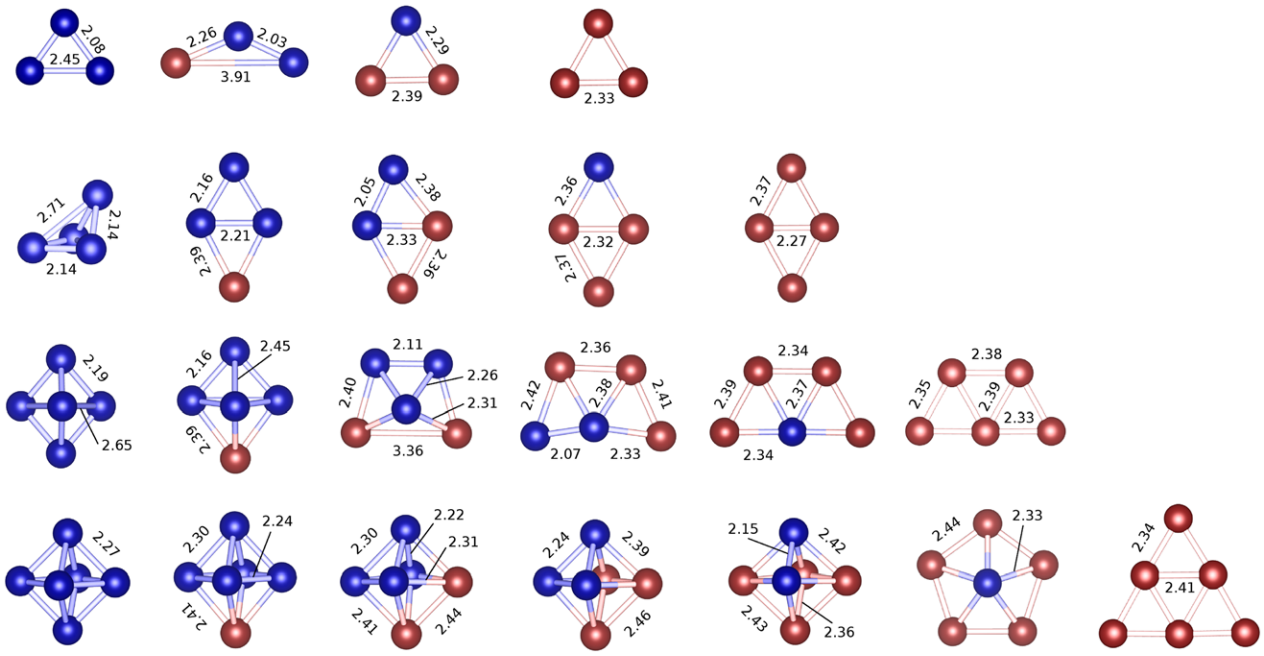

Figure 1. Ground-state *ab initio* configurations of $Co_{n-m}Cu_m$ clusters for sizes $n = 3$–6 (rows) and $m = 0$–6 (columns). Co atoms are given as (dark) blue balls and Cu atoms as (clear) red balls. Most relevant bond lengths are indicated in units of Å. For fixed cluster sizes, from right to left, we observe a 2D to 3D geometric transition at some point as the number of Co atoms increases. The pristine Co_n ($m = 0$) are cage-like 3D clusters for $n \geq 4$, while the pristine Cu_n ($m = n$) clusters in this series are all planar. Figure adapted from [3].

works involving the description of cobalt–copper clusters using density-functional tools. Specifically, a recent work by Aguilera-Granja *et al* [15], describing the particular case of 12 atoms, $Co_{12-m}Cu_m$, for all stoichiometries ($0 \leq m \leq 12$), will serve as a special benchmark for our proposal of the magnetic properties of Co–Cu clusters of up to 20 atoms.

As concerns the approach taken by us, namely, to verify the suitability of the jellium deformable model to describe the magnetic properties of Co–Cu clusters derived from first-principle calculations, we should mention other alternative approaches for the (also transition metal) Ni case [16], where an incipient work in that direction was conducted through a simple electronic-shell model to estimate the magnetic moments of Ni clusters. Moreover, a similar approach for the same case of Ni clusters was also worked out through a tight-binding description [17]. These pioneer works pointed out the important task of predicting the magnetism in finite clusters, as the first-principle calculations for each case would demand an extraordinary numerical effort.

2. Previous results from two to six atoms

In our earlier work [3], we have performed density-functional calculations using the generalized gradient approximation (GGA) for cobalt–copper ferromagnetic clusters with few atoms, $n = 2$–6, assuming the 3d and 4s as the valence electrons. The Perdew–Burke–Ernzerhof (PBE) expression [18] for the exchange–correlation potential was used within the VASP algorithm [19–21]. A summary of that work is given in figure 1 and table 1.

One of the outcomes of this study is that the ground-state configurations exhibit a 2D to 3D geometric transition when substituting Cu by Co atoms. This behavior comes from the partially filled $3d^8 4s^1$ shell of Co atoms and the completely filled $3d^{10} 4s^1$ shell of Cu atoms. The density-functional orbital hybridization keeps the inner core 3d occupancy of the clusters almost identical to that in the atoms because

Table 1. Ground-state *ab initio* properties of cobalt–copper clusters, from trimers to hexamers: point symmetry groups; binding energies E_b (in eV/atom); total magnetic moments M (in μ_B). One magnetic case (Co_1Cu_2) differs from the ultimate jellium model, as indicated in parentheses. Values compiled from [3].

Cluster	Symm.	E_b (eV)	M (μ_B)
Co_3	C_{2v}	1.86	7
Co_2Cu_1	—	1.63	5
Co_1Cu_2	C_{2v}	1.31	1(3)
Cu_3	D_{3h}	1.22	1
Co_4	D_{2d}	2.33	10
Co_3Cu_1	C_{2v}	2.07	6
Co_2Cu_2	—	1.84	4
Co_1Cu_3	C_{2v}	1.60	2
Cu_4	D_{2h}	1.58	0
Co_5	D_{3h}	2.61	13
Co_4Cu_1	C_{2h}	2.37	9
Co_3Cu_2	C_{2v}	2.13	7
Co_2Cu_3	—	1.96	5
Co_1Cu_4	C_{2v}	1.81	3
Cu_5	C_{2v}	1.71	1
Co_6	O_h	2.98	14
Co_5Cu_1	O	2.71	12
Co_4Cu_2	—	2.51	10
Co_3Cu_3	C_3	2.31	8
Co_2Cu_4	—	2.10	6
Co_1Cu_5	C_5	1.98	2
Cu_6	D_{3h}	1.90	0

of strong localization effects (tested by Bader and Voronoi charge analyses). At the same time, such mixing allows the surroundings of cobalt atoms to be more flexible for chemical bonding, leading to tridimensionality, as demonstrated in [3]. Binding energies per atom, $E_b = [(n - m)E_{Co} + mE_{Cu} - E_{GGA}]/n$, increase with the presence of Co atoms because of a stronger Co–Co bonding (in this respect, we notice the concomitant shorter Co–Co bond lengths in figure 1). This fact also leads to Co clumping in the clusters, which implies a tendency for segregation processes in the thermodynamic limit, as is indeed observed in cobalt–copper melt-spun magnetic alloys [22]. Such segregation is closely tied to the giant magnetoresistance phenomena observed in these novel materials [23].

As is seen from table 1, the magnetic moments obtained in [3] follow an interesting trend: whilst free copper atoms are nonmagnetic, the pristine Cu_n clusters have either 0 or 1 μ_B for even/odd clusters. This staggering magnetic order effect has already been explained [24] in terms of closed/open shells of the ground-state molecular orbital configurations. When substituting a copper by a cobalt atom within a cluster, an increase of 2 μ_B per Co atom normally occurs, because of the unfilled $(3d^5_\uparrow)(3d^3_\downarrow)$ Co atomic shells, which remain almost equally populated in the clusters due to charge localization effects. This rule has one exception, the Co_1Cu_2 cluster, which will be studied below.

Now, every time a 2D to 3D geometric transition occurs there is a change of 4 μ_B in the magnetic moment of the sequence, as is seen from Co_3Cu_1 to Co_4 ($n = 4$), Co_4Cu_1 to Co_5 ($n = 5$), or Co_1Cu_5 to Co_2Cu_4 ($n = 6$), comparing the results in figure 1 and in table 1. The magnetic moments obtained from this GGA–PBE approach [3], at the ground-states, were found to coincide with most of the results of the ultimate jellium model, as explained in section 3.

3. The ultimate jellium model

The ultimate many-body jellium model [4, 5] is a model which replaces the discrete ions by a positive background charge, which itself deforms to adapt its shape and density profile to the electronic cloud point-to-point. In this approach, the minimum of energy is obtained for a neutral deformable electron gas by solving the Kohn–Sham equations, giving thus a definite shape according to the exchange–correlation potential of N electrons. Their spin magnetic moment results can be understood in terms of the occupancy of the s, p_x, p_y, p_z, etc, single particle wavefunctions of the spherical system. Although the p levels in the spherical system are degenerate, in deformable systems the Jahn–Teller effect splits them unless the ℓ shell is full. The orbital number, ℓ, is no longer a good quantum number, but still can be used as a reference for the symmetries of the unperturbed system.

There are two types of result in this model, depending on the dimensionality of the ground-state configuration. For 2D geometrical configurations (obtained by imposing the solution in a strong external 2D surface potential), the filling sequence of the single particle levels for $n = 2$–6 electrons goes as follows: $1s^2$, $1s^2p_x$, $1s^2p_x^2$, $1s^2p_x^2\,p_y$, $1s^2p_x^2\,p_y^2$, which says, in passing, that systems with $n = 7$ or more electrons cannot be two-dimensional, because the 2D p-shell is fully occupied. On the other hand, for 3D geometrical configurations (obtained for free-standing clusters), we have an alternative filling sequence, for $n = 2$–8 electrons: $1s^2$, $1s^2p_x$, $1s^2p_x\,p_y$, $1s^2p_x\,p_y\,p_z$, $1s^2p_x^2\,p_y\,p_z$, $1s^2\,p_x^2\,p_y^2\,p_z$, $1s^2\,p_x^2\,p_y^2\,p_z^2$. Magnetic moments built up according to these filling sequences are collected in table 2.

Table 2. Magnetic moments (in μ_B) for the p-shell in the ultimate jellium model, where n is the number of valence electrons, for 2D and 3D geometrical arrangements.

n	2	3	4	5	6	7	8
2D	0	1	0	1	0	—	—
3D	0	1	2	3	2	1	0

With these arguments, we expect the magic case $n = 8$ to be spherically symmetric because of a full 3D p-shell, as is indeed obtained in [4]. Another magic case is expected for $n = 18$, where we would have a fully occupied d-shell, like in the series $1S^2\ 1P^6\ 1D^{10}$, which is, however, not spherically symmetric because of a strong hybridization of the 1d and 2s levels (although it has a quasi-degenerate spherical isomer). Instead, the cases $n = 19$ and 20 are found to be spherically symmetric [4], where the contribution from 2s orbitals comes in. Incidentally, the filling sequence of the spherical jellium model shells for higher occupation levels is given by $1S^2\ 1P^6\ 1D^{10}\ 2S^2\ 1F^{14}\ 2P^6$ etc.

We notice that our GGA magnetic moment results for Co–Cu clusters (cf table 1) match those from the ultimate jellium model if one attributes the contribution of the 4s valence electrons of the atoms from table 2, checks the dimensionality from figure 1, and adds 2 μ_B per each Co atom in the cluster. This rule, as said, has one exception: Co_1Cu_2.

4. Prediction for 7–20 atoms

One of the main purposes of this work is to make a prediction of the magnetic moments for cobalt–copper clusters of up to twenty atoms, based on the results we have at hand. This limit prevents occupancy of the $1F^{14}$ series, which we shall not discuss here. Based on arguments of dimensionality and charge localization, our former GGA results [3] have been combined with other DFT studies, from Jaque *et al* [24] for pure copper clusters, and from Datta *et al* [25] for pure cobalt clusters. The resulting scheme is depicted in figure 2 for all stoichiometries.

Concerning our previous work, for $n = 2$–6 atoms (black dots), taking out the exotic Co_1Cu_2 case, all the other results follow straight lines, increasing by 2 μ_B per Co-contribution, with the exceptional 4 μ_B jumps for $n = 4$–6, where the geometric transitions from 2D to 3D configurations take place [3]. To be consistent, we shall assume that $M = 3$ μ_B is the best guess for the spin moment of the Co_1Cu_2 cluster (indicated by a black dotted line in figure 2). In favor of this assumption, we mention that Co_1Cu_2 has a 3 μ_B first isomer, which is very close in energy ($\Delta E = 30$ meV) to its 1 μ_B ground-state [3].

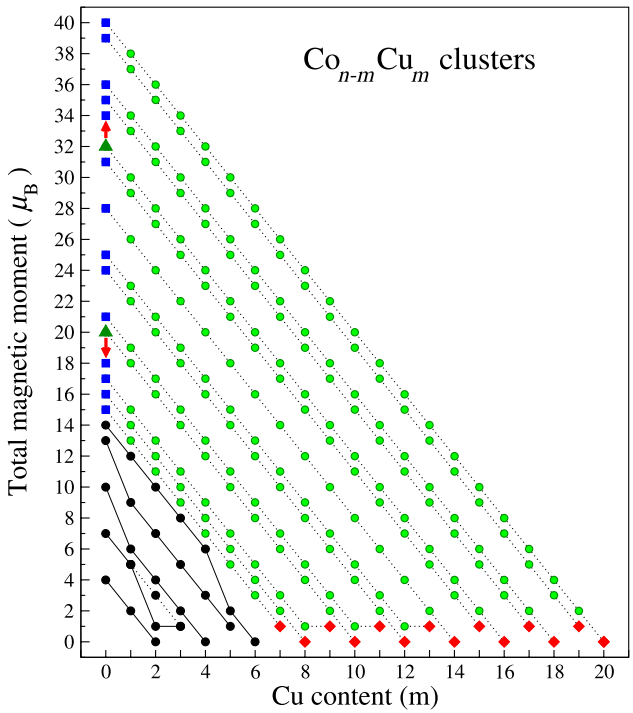

Figure 2. Total magnetic moments of $Co_{n-m}Cu_m$ neutral clusters for up to 20 atoms. Clusters of equal sizes (n) are joined with lines to guide the eye. Black circles: from Pérez *et al* [3]; see that Co_1Cu_2 was corrected to have 3 μ_B (joined by a black dotted line). Red diamonds: pristine Cu_n clusters from Jaque *et al* [24]; observe the staggering order for even/odd Cu_n clusters. Blue squares: pristine Co_n clusters from Datta *et al* [25]; two exceptional cases, Co_{10} and Co_{16}, do not match this proposal, first isomers were taken instead (green triangles), their ground-state moments are indicated by red vertical arrows. Green circles: predicted magnetic moments from $n = 7$ to 20 atoms for all stoichiometries according to this work.

On the other hand, we have the valuable results for pure copper clusters from Jaque *et al* [24], where the even–odd staggering order follows from closed/open shells of the ground-state cluster configurations. We have verified them up to $n = 7$, using VASP calculations. We shall therefore adopt such a staggered magnetic sequence (without explicit calculation) up to $n = 20$ atoms, as given by the red diamonds in figure 2.

The values of the magnetic moments for pristine cobalt neutral clusters were initially taken from an independent GGA calculation, by Datta *et al* [25]. We have verified them thoroughly with our own GGA calculations using VASP, with the same accuracy as in [3]. For two exotic clusters, Co_{10} and Co_{16}, their values were taken from their first isomers instead, to fit the figure. This is indicated by the green triangles and red vertical arrows pointing toward the Datta ground-state values (blue squares). These two cases will be extensively discussed below. We notice from this scheme that there is only one way to join the pristine clusters from both sides, starting from the pure copper clusters, and imposing the rule of 2 μ_B increase per Co-contribution, to match the pure cobalt results. The predicted magnetic moments for all stoichiometries are given by the intermediate green circles joined by green dotted lines in figure 2.

We have, at least, one *ab initio* GGA calculation in the particular case of $n = 12$ atoms to compare with. The work by Aguilera-Granja *et al* [15] for $Co_{12-m}Cu_m$ shows a strong relative success with our proposed solution. Their magnetic moments coincide with our results, as given in figure 2, for three geometric configurations they have considered (hexagonal compact, planar icosahedron, and buckled biplanar). However, their work fails to confirm our prediction in the fourth icosahedral minus an (apex) atom configuration. In that case, their moments coincide at the extremes, except for the intermediate cases $m = 6$–8, where the magnetic moments are given by 10, 8 and 6 μ_B, respectively. There is coincidence at least in the majority of cases.

In the same spirit as the comparison with the $1S^2$ $1P^6$ series of the jellium model, discussed in the previous section, we propose here that the d-shell filling for the pristine cobalt clusters, from $n = 9$–20 atoms, follows that given in table 3. Most important here is the situation of unpaired states. We see that the first six clusters tend to reduce and the last six to increase the Co core magnetic moments. In other words, the first half of this cluster series has 4s electrons that align antiferromagnetically and the second half align ferromagnetically. Clusters with even numbers of atoms do not change the core contribution. However, the two exceptional cases discussed above, Co_{10} and Co_{16}, subtract/add 2 μ_B, respectively. These two irregular clusters are important clues in the comparison with experiments, which is the subject of section 5.

5. Comparison with experiments

Let us compare our prediction with some recent experimental data. Magnetic moments for neutral cobalt clusters were reported by Knickelbein [6], using a molecular beam deflection method. In figure 3 we have combined these measurements with our previous results, for $n = 2$–6 atoms, and the new VASP calculations for neutral cobalt clusters, from $n = 7$–20 atoms. With respect to the latter, we have verified all the ground-state results previously published by Datta *et al* [25]. Starting from their *xyz*-positions[4], we have tested the stability of these results with a fitted many-body potential through a specially designed Monte Carlo calculation. See the appendix for further details.

It is known that small clusters exhibit very strong finite-size effects in their magnetic properties. This is the case in this study, with the calculated moments oscillating between the bulk limit and the experimental results. Still, one notices from figure 3 a striking behavior of the two exotic cobalt clusters, Co_{10} and Co_{16}. One sees, markedly, the dip for Co_{10} and the maximum for Co_{16} in figure 3, whose trends are reproduced by our GGA calculations. This means that the ultimate jellium model cannot explain all the subtleties of these clusters. In particular, there is no way to dovetail the magnetic behavior of Co_{10} and Co_{16} through the normal

[4] We thank Dr Mukul Kabir (MIT) for kindly sending their results [25] for the atomic positions.

Table 3. Proposed filling of the 1D series (and 2S) for the pristine Co_n neutral clusters, from $n = 9$ to 20 atoms. Paired electrons are indicated in parentheses; 'core' means the moment contribution from the $(3d^5_\uparrow)(3d^3_\downarrow)$ Co cores; M is the total magnetic moment. The first six clusters tend to diminish the core moments and the last six tend to increase them. Even clusters have the same moments as the core contributions, except for $n = 10$ and 16 (starred), where a variation of 2 μ_B is observed.

n	1D series	Core (μ_B)	M (μ_B)
9	↓	18	17
10	↓↓	20	18*
11	(↓↑) ↓	22	21
12	(↓↑)(↓↑)	24	24
13	(↓↑)(↓↑) ↓	26	25
14	(↓↑)(↓↑)(↓↑)	28	28
15	(↑↓)(↑↓)(↑↓) ↑	30	31
16	(↑↓)(↑↓)(↑↓) ↑↑	32	34*
17	(↑↓)(↑↓)(↑↓)(↑↓) ↑	34	35
18	(↑↓)(↑↓)(↑↓)(↑↓)(↑↓)	36	36
19	(↑↓)(↑↓)(↑↓)(↑↓)(↑↓) $2s^1$ ↑	38	39
20	(↑↓)(↑↓)(↑↓)(↑↓)(↑↓) $2s^2$ (↑↓)	40	40

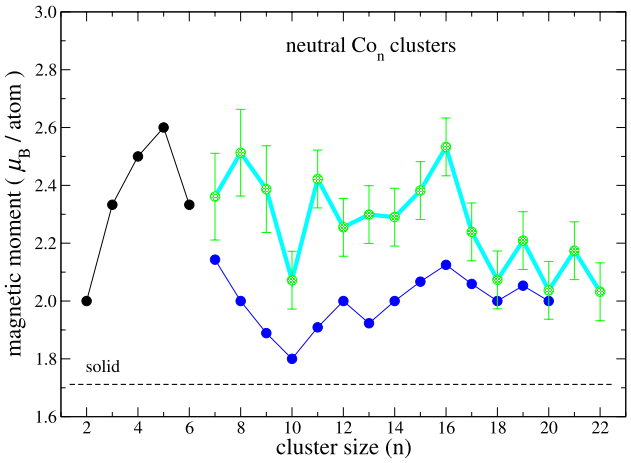

Figure 3. Magnetic moment per atom for neutral cobalt clusters Co_n. Black points: previous GGA results for $n = 2$–6 atoms [3]. Blue points: new GGA results for $n = 7$–20 atoms (same values as in [25]). Green points (with error bars): experimental results for $n = 7$–22 atoms, obtained by Knickelbein [6]. The dashed line is the bulk limit (1.72 μ_B/atom).

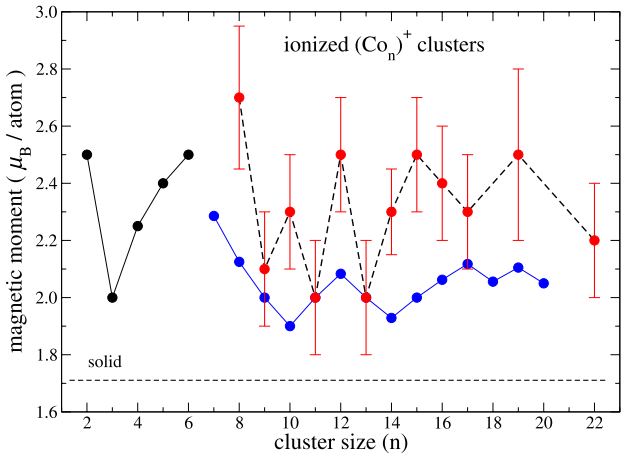

Figure 4. Magnetic moment per atom of singly ionized cobalt clusters Co_n^+. Black points: new GGA results for $n = 2$–6 atoms. Blue points: new GGA results for $n = 7$–20 atoms. Red points (with error bars): as revealed by XMCD for free magnetic ionized Co_n^+ clusters, for $n = 8$–22 atoms, from Peredkov *et al* [7].

filling of the d-shell, as described in section 4. These two cases are known to be highly deformed (strongly hybridized) and very far from the unperturbed spherical wavefunctions we are using to describe them. Most certainly, the physical ingredient entering into this distortion is the Jahn–Teller coupling and/or the spin–orbit splitting. Either contribution tends to deform the spherical situation, specially for unfilled ℓ-shells.

We take a step forward and make a similar comparison for ionized cobalt clusters with a recent experiment, performed by Peredkov *et al* [7]. The result is given in figure 4. The comparison is quite similar to those above, but worse, with higher values for the magnetic moments (on average) and larger fluctuations in the experimental data. The calculated values seem to always be underestimated. We also see this time that the tendency to the bulk limit goes down slowly. Many questions arise concerning the lack of fitting of such new results. Among them, we may mention the possible contribution of the magnetic anisotropy energy (MAE) [26], a possible superparamagnetic behavior versus locked-moment isomers [6], and possible shake-up and shake-off effects from the ionization process [27]. These are important features in order to extract the intrinsic value of the spin magnetic moment from its temperature dependence, which must be also well separated from its (small) orbital moment contribution.

Because of charge neutrality, we are not able to compare this case with the ultimate jellium model. The new GGA calculations for ionized cobalt clusters were obtained starting from the same configurations as for the corresponding neutral cases, by taking out one electron from the cluster, and relaxing them using VASP calculations. The results were assessed with the same Monte Carlo approach and many-body potential as before (see the appendix), to verify their stability. This approach was developed as a genetic algorithm for finding candidates of lower binding energies, which were further optimized to the lowest energy structures using the VASP package based on density-functional theory.

6. Discussion

Two groups of exotic cobalt–copper clusters were discussed in the text, in the comparison with the ultimate jellium model.

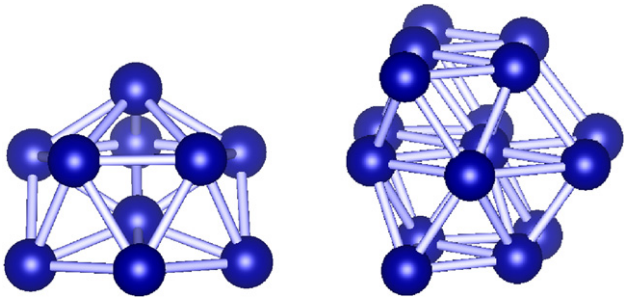

Figure 5. The ground-state geometric configurations found with GGA calculations, for Co_{10} (left) and Co_{16} (right). The first is a tricapped pentagonal bipyramid, with $M = 18\ \mu_B$, while the second is a stacked three-layered truncated hexagonal configuration, with $M = 34\ \mu_B$.

The first one was related to Co_1Cu_2, which did not fit the expected 2 μ_B increase by Co-contribution. (Another cluster, Co_4Cu_1, indicated as such in [3], is not exotic because it is on the verge of the 2D to 3D geometric transition.) The Co_1Cu_2 cluster might be exotic (with 1 μ_B) because one of the 4s valence electrons is coupled antiferromagnetically to the Co core. Or it might be regular, with parallel coupling (namely, 3 μ_B), in which case we must correct its GGA result, as we did in figure 2. This is strongly advised because its first isomer is regular and quasi-degenerate ($\Delta E = 30$ meV) with its putative ground-state. In any case, we took for granted this antiparallel coupling tendency, when one Co atom stands alone in the cluster, to propose the magnetic behavior of Co_1Cu_{n-1} for $n = 9$, 11 and 13, as seen in figure 2.

The second exotic group is related to the anomalies of Co_{10} and Co_{16}. These two pure cobalt clusters are highly deformed in the language of the ultimate jellium model. In this context, the nonspherical Co_{10}, for example, is interpreted as a combination of two magic clusters, Co_2 and Co_8. In fact, as given by our GGA results (see figure 5), the ground-state of Co_{10} is more like a hemisphere, while the ground-state of Co_{16} is more hexagonal and far from being spherical.

Finally, the comparison with the only GGA *ab initio* case we found for the whole stoichiometric series, the case of 12 atoms by Aguilera-Granja *et al* [15], demonstrated a nice coincidence of our proposal with first-principle calculations, at least in the majority of the configurations calculated. Such a coincidence corroborates the quality of our proposal. Such a proposal is based on the strong 3d charge localization of the cobalt and copper atoms in the constituted clusters, leaving no means for antiferromagnetic couplings, as was predicted by Lu *et al* [14], and corroborated by Aguilera-Granja *et al* [15].

In conclusion, we studied the magnetic properties of small Co–Cu clusters using various approaches. A connection of our first-principle GGA results with those of the ultimate many-body jellium model has been established, in two parts. First, from $n = 2$ to 8 atoms, involving the $1S^2\ 1P^6$ shells of the unperturbed spherical wavefunctions. Second, from $n = 9$ to 20 atoms, involving the $1D^{10}\ 2S^2$ shells, where we developed a scheme to predict the magnetic behavior for all stoichiometries. For that purpose, we used other independent density-functional results for the pristine cases, together with a Monte Carlo approach based on a many-body fitted potential, to verify some of these results. We found two exotic clusters, Co_{10} and Co_{16}, which do not obey the rules of this prediction. Our explanation of this fact is a sort of nonspheroidicity, or strong hybridization, rendering the description in terms of unperturbed wavefunctions, with a fixed orbital number ℓ, completely obsolete.

Furthermore, the comparison with experiments reveals that the true spin-polarized electron density distribution associated with each ionic configuration, as obtained from first-principle calculations, is required when further details are needed. We also feel that future studies will have to make a difference between neutral and ionized clusters, extending these results to cationic and anionic cases.

Acknowledgments

We acknowledge financial support from CNPq (Brazil) Project CIAM 490891/2008-0, FONDECYT-Chile Grant No. 1100365, MINECON-Chile Grant No. ICM P10-061-F and Project No. FB0807.

Appendix

The empirical many-body tight-binding pseudopotential, $E_p = \sum_i (E_B^i + E_R^i)$, as reported by Cleri and Rosato [28], was used with a cut-off radius at the fifth neighbors. It consists of an attractive band energy interaction given by

$$E_B^i(r_{ij}) = -\left[\sum_j \xi_{\alpha\beta}^2 \exp\left\{-2q_{\alpha\beta}(r_{ij}/r_0^{\alpha\beta} - 1)\right\}\right]^{1/2},$$

where r_{ij} is the interatomic distance between atoms i and j, $r_0^{\alpha\beta}$ is the first-neighbor distance in the lattice $\alpha\beta$, ξ is an effective hopping integral, and q describes its dependence on the relative interatomic distance. Both q and ξ are assumed to depend only on the interacting atomic species α and β. To ensure stability, a repulsive term is needed and this is normally assumed to be pairwise and short-ranged, better described by a sum of Born–Mayer ion–ion repulsive potentials

$$E_R^i(r_{ij}) = \sum_j A_{\alpha\beta} \exp\left\{-2p_{\alpha\beta}(r_{ij}/r_0^{\alpha\beta} - 1)\right\},$$

whose origin can be traced back to the increase of kinetic energy of the conduction electrons. Traditionally, the free parameters, A, ξ, p, q, and r_0, are fitted to experimental values of the cohesive energy E_p, the lattice parameters, and the elastic constants for each crystalline system. The values that we use with Co–Cu clusters are those of the bulk systems, described in table A.1.

Table A.1. Empirical parameters for Cu (fcc) and Co (hcp) systems.

Type	A (eV)	ξ (eV)	p	q	r_0 (Å)
Cu (fcc)	0.0855	1.224	10.960	2.278	2.556
Co (hcp)	0.0950	1.488	11.604	2.286	2.480

One notices that this empirical potential is spherically symmetric, depending only on the radii (and nonmagnetic), whence its minimal-energy solutions will tend to be so. We have used it to run simulated annealings with the Monte Carlo technique at high temperatures, reducing the temperature, and collecting the information on each previous configuration until the system is sufficiently quenched. We employed this approach prior to the VASP calculation as a successful search mechanism for the different minimal-energy cluster configurations.

References

[1] Ferrando R, Jellinek J and Johnston R L 2008 *Chem. Rev.* **108** 845
[2] Baibich M N, Broto J M, Fert A, Nguyen Van Dau F, Petroff F, Etienne P, Creuzet G, Friederich A and Chazelas J 1988 *Phys. Rev. Lett.* **61** 2472
[3] Pérez M, Muñoz F, Mejía-López J and Martínez G 2012 *J. Nanopart. Res.* **14** 933
[4] Koskinen M, Lipas P O and Manninen M 1995 *Z. Phys.* D **35** 285
[5] Kolehmainen J, Häkkinen H and Manninen M 1997 *Z. Phys.* D **40** 306
[6] Knickelbein M B 2006 *J. Chem. Phys.* **125** 044308
[7] Peredkov S, Neeb M, Eberhardt W, Meyer J, Tombers M, Kampschulte H and Niedner-Schatteburg G 2011 *Phys. Rev. Lett.* **107** 233401
[8] Dunlap B I 1990 *Phys. Rev.* A **41** 5691
[9] Reddy B V, Khanna S N and Dunlap B I 1993 *Phys. Rev. Lett.* **70** 3323
[10] Jena P and Castleman AW (ed) 2010 *Nanoclusters: A Bridge Across Disciplines* (Amsterdam: Elsevier)
[11] Lorke A, Winterer M, Schmechel R and Schulz C (ed) 2012 *Nanoparticles from the Gas Phase* (*Springer Series NanoScience and Technology*) (Berlin: Springer)
[12] Wang J L, Wang G, Chen X, Lu W and Zhao J 2002 *Phys. Rev.* B **66** 014419
[13] Ju S P, Lo Y C, Sun S J and Chang J G 2005 *J. Phys. Chem.* B **109** 20805
[14] Lu Q L, Zhu L Z, Ma L and Wang G H 2005 *Chem. Phys. Lett.* **407** 176
[15] Aguilera-Granja F, Torres M B, Vega A and Balbás L C 2012 *J. Phys. Chem.* A **116** 9353
[16] Fujima N and Yamaguchi Y 1996 *Phys. Rev.* B **54** 26
[17] Bouarab S, Vega A, López M J, Iñiguez M P and Alonso J A 1997 *Phys. Rev.* B **55** 13279
[18] Perdew J P, Burke K and Ernzerhof M 1996 *Phys. Rev. Lett.* **77** 3865
[19] Kresse G and Hafner J 1994 *J. Phys.: Condens. Matter* **6** 8245
[20] Kresse G and Furthmüller J 1996 *Phys. Rev.* B **54** 11169
[21] Kresse G and Joubert D 1999 *Phys. Rev.* B **59** 1758
[22] Miranda M G M, Estévez-Rams E, Martínez G and Baibich M N 2003 *Phys. Rev.* B **68** 014434
[23] Miranda M G M, da Rosa A T, Hinrichs R, Golla-Schindler U, Antunes A B, Martínez G, Estévez-Rams E and Baibich M N 2006 *Physica* B **384** 175
[24] Jaque P and Toro-Labbé A 2004 *J. Phys. Chem.* B **108** 2568
[25] Datta S, Kabir M, Ganguly S, Sanyal B, Saha-Dasgupta T and Mookerjee A 2007 *Phys. Rev.* B **76** 014429
[26] Glaser L, Chen K, Fiedler S, Wellhöfer M, Wurth W and Martins M 2012 *Phys. Rev.* B **86** 075435
[27] Svensson S, Eriksson B, Martensson N, Wendin G and Gelius U 1988 *J. Electron Spectrosc. Relat. Phenom.* **47** 327
[28] Cleri F and Rosato V 1993 *Phys. Rev.* B **48** 22